c.2

NACA

RESEARCH MEMORANDUM

ANALYTICAL INVESTIGATION OF FLOW AND HEAT TRANSFER IN COOLANT PASSAGES OF FREE-CONVECTION LIQUID-COOLED TURBINES

By E. R. G. Eckert and Thomas W. Jackson

Lewis Flight Propulsion Laboratory
Cleveland, Ohio

NATIONAL ADVISORY COMMITTEE
FOR AERONAUTICS
WASHINGTON
July 18, 1950

NATIONAL ADVISORY COMMITTEE FOR AERONAUTICS

RESEARCH MEMORANDUM

ANALYTICAL INVESTIGATION OF FLOW AND HEAT TRANSFER IN COOLANT PASSAGES OF FREE-CONVECTION LIQUID-COOLED TURBINES

By E. R. G. Eckert and Thomas W. Jackson

SUMMARY

Gas turbines provided with free-convection cooling have rotating blades with cylindrical holes that are closed on top of the blade and connected with the fluid supply at the blade root. In the design of such blades, an important question arises as to what minimum diameter a hole of a certain length can be drilled without endangering the circulation of the cooling liquid in it. An approximate answer to this problem is obtained by calculating the thickness of the heated boundary layer that builds up around the cylindrical surface of a hole with large diameter.

Numerical evaluations of the results of these calculations for a sample turbine and comparisons with test results show that in small holes such as would be required in the leading and trailing edges of turbine blades, the circulation and the cooling effect is appreciably impaired. The circulation and the cooling effect in these holes can be considerably improved when a connection is provided on top of the blades between the small holes and the larger holes, which can be located in the central portion of the turbine blade.

In the boundary-layer calculations, the effect of the Coriolis forces on the movement of the liquid in the rotating holes was neglected. The magnitude of the Coriolis forces relative to the centrifugal forces was calculated and the influence of the secondary movement set up by the Coriolis forces on the cooling effect was estimated by comparison with test results on inclined surfaces in gravitational free-convection heat transfer.

INTRODUCTION

Liquids are more effective coolants than gases because of their better conductivities. Gas turbines can therefore be operated with higher gas temperatures and, accordingly, with better efficiency and greater power per unit gas flow when they are cooled with liquids.

The most critical parts to be cooled in gas turbines are the rotating blades. In using liquids to cool the blades, the very large free-convection currents that are generated by the centrifugal forces can be used. This cooling method was first proposed by E. Schmidt (reference 1). Experiments at the NACA Lewis laboratory proved its effectiveness. Figure 1 shows this cooling arrangement for a turbine blade according to the proposal of Schmidt. The cooling liquid fills up the cylindrical holes of circular cross section inside the blade. The holes are closed on top and connected at the bottom with the fluid supply.

When the blades are heated by hot gases, the heat penetrates through the solid material of the blades to the surface of the holes, where it heats a thin layer of liquid adjacent to the surface. When the liquid layer is heated, the density in the layer becomes smaller than the density in the cooler liquid core near the center of the hole. In the rotating turbine, the fluid in the hole is subjected to a centrifugal acceleration equal to $r\omega^2$. (All symbols used in this report are defined in appendix A.) The centrifugal forces $\rho r\omega^2$ per unit volume are smaller in the heated layer (boundary layer) because of its smaller density ρ and cause this layer to flow toward the axis of rotation. The hot fluid leaving the hole in this way has to be replaced by cool fluid flowing outward in the core. The velocity profile in a cross section of the hole must therefore have a shape similar to that shown in the central hole of figure 1.

The circulation of the liquid in a hole will be good as long as the cross section of the core is large as compared with the cross section of the heated boundary layer. When the diameter of a hole is small as compared with its length, then the space left for the core will become too small and the circulation will diminish. For holes with very small diameters the flow may break down entirely.

On the other hand, it is necessary to arrange as many holes as possible in the blade in order to minimize the thickness of solid material through which the heat must flow. If the heat has to flow over a long distance within the solid material, the blade cannot be cooled effectively. An analytical investigation of the problems arising in connection with this cooling method was conducted at the NACA Lewis laboratory and is presented herein. This analysis investigates: (1) the smallest diameter hole that can be made without endangering the circulation of the liquid, and (2) methods of improving the circulation in a small-diameter hole.

METHOD OF ANALYSIS

A hole of very large diameter as compared with its length is first considered. In this hole, the cross-sectional area of the core of the liquid is very large compared with the cross-sectional area of the heated layer adjacent to the wall and consequently the velocity of the fluid in the core is very small. By decreasing the diameter of the hole, the flow in the heated layer and its thickness will change; however, as long as the cross section of the core is considerably larger than the cross section of the layer, the change will be negligible. Only when both areas are comparable in magnitude will the circulation start to decrease appreciably. Consequently, if it is possible to calculate the thickness of the heated layer for a very large hole, it is possible to estimate at what diameter the circulation will start to decrease appreciably.

As long as the length of the hole is small compared with the diameter of the turbine wheel, so that the radius in the expression for the centrifugal forces may be replaced by some average value, the conditions for the flow in such a hole are practically the same as the conditions of free-convection flow in a vertical stationary cylinder that is filled with liquid and whose walls are heated. The bottom of the cylinder is closed and the top is open and connected to a liquid supply. A liquid film around the inside of the wall will be heated and rise by its buoyancy forces. Cold liquid from the supply on top will replace the warm liquid film leaving the cylinder. The centrifugal force $\rho r\omega^2$ that causes the circulation of the cooling liquid in the turbine blade is replaced by the gravitational force ρg (per unit volume) in the equipment just described.

The flow conditions in a hole with a very large diameter are the same as on a vertical-plane plate. Considerable information exists on gravitational free-convection flow on a vertical wall. It is characterized by a dimensionless value, the Grashof number, in the same way that forced-convection flow is characterized by the Reynolds number. In comparing the gravitational free-convection flow with the centrifugal flow, the acceleration due to gravity g has to be replaced by the centrifugal acceleration $r\omega^2$ in the expression for the Grashof number. When the Grashof numbers in both systems have the same value, the results obtained theoretically or experimentally on a gravitational flow can be transferred to the flow in the turbine-blade holes.

A boundary layer builds up on the surface of the vertical wall in free-convection flow in much the same manner as in forced-convection flow. The flow within the boundary layer is laminar or turbulent, depending on the magnitude of the Grashof number. The transition takes place at a Grashof number between 10^9 and 10^{10}. The thickness of the laminar boundary layer, as well as the temperature and velocity profiles within this layer, and the heat transfer were measured by E. Schmidt and W. Beckmann (reference 2) and compared with values that they calculated with the help of E. Pohlhausen. The Grashof numbers in the holes of liquid-cooled turbine blades, based on the length of the holes, are in the approximate range of 10^{12} to 10^{15}. The boundary layer is therefore expected to be turbulent over almost the whole length of the holes. Some measurements exist on the heat transfer in the turbulent region, but they cover only a range of Grashof numbers from 10^9 to 10^{12} (references 3 and 4). Nothing, however, is known on the thickness of the turbulent boundary layer or on the velocity and temperature profiles in this layer.

Insufficient information is available on turbulent forced flow to calculate exactly velocity profiles and boundary-layer thicknesses. In addition, practically no information is available on the mechanism of free-convection flow in the turbulent range. It is therefore possible to make only approximate calculations for the boundary-layer thickness in this region. The calculations using the Kármán momentum equation of the boundary layer (reference 5) and an analogous heat-flow equation are presented in the section DETERMINATION OF TURBULENT FREE-CONVECTION BOUNDARY LAYER. Similar calculations were made by Squire (presented in reference 6) for the laminar free-convection boundary layer and his results satisfactorily checked the results of the exact theory and of experiments.

So far only the centrifugal forces in the fluid that fills the holes have been considered. It is known, however, that in studying the motion relative to a rotating system, two kinds of forces have to be considered, the centrifugal and Coriolis forces. The Coriolis forces set up a secondary movement in the liquid circulating in the holes of a rotating turbine blade that is superimposed on the movement generated by the centrifugal forces. The relative magnitude of the centrifugal and Coriolis forces is considered and the secondary movement described in a subsequent section of the paper.

DETERMINATION OF TURBULENT FREE-CONVECTION BOUNDARY LAYER

Derivation of Boundary-Layer Equations

If a stationary, plane, vertical wall is heated to a temperature higher than its surroundings, the layer of fluid adjacent to the wall is heated by conduction from the wall. In this way, buoyancy forces are generated that cause this layer to flow in an upward direction. A boundary layer is built up that begins with zero thickness at the lower end of the vertical wall and increases in thickness in the upward direction. The boundary layer becomes turbulent, depending on the critical Grashof number, at a certain distance from the lower end of the wall. The distance measured vertically from the lower end of the plate is called x and the distance normal to the plate is y. In order to determine the boundary-layer thickness for steady state, a small stationary volume element in the turbulent region of the boundary layer is considered. Figure 2 shows this volume element. The dimensions of the element are dx along the plate and l normal to it. The length l should be larger than the boundary-layer thickness δ. Considering two-dimensional flow, the dimension of the volume element normal to the plane of figure 2 may be considered to be unity. The upward velocity of the fluid in plane 1-1 at a distance y from the surface of the wall is u. Then the mass flow through a small area with a width dy is $\rho u\,dy$ and the flow of momentum in the x-direction is $\rho u^2\,dy$. The momentum flow in the x-direction entering the volume element through plane 1-1 is

$$\int_0^l \rho u^2\,dy$$

In progressing to plane 2-2, the momentum flow changes by

$$\frac{d}{dx}\left(\int_0^l \rho u^2\,dy\right)dx$$

In general, the mass flow entering the volume element through plane 1-1 is different from the mass flow leaving it through plane 2-2, which means that fluid enters or leaves the

volume element through the plane parallel to the wall at a distance l. Inasmuch as it is assumed that the velocity in the x-direction can be neglected outside the boundary layer, no momentum in the x-direction is carried through the plane.

The rate of change of momentum must be in equilibrium with the forces acting in the x-direction on the fluid within or on the surface of the volume element considered. A shearing stress τ_w acts on the wall. The force connected with this stress is $\tau_w \, dx$. No shearing stress occurs on the surface of the volume element that is parallel to the wall and at a distance l from it because outside the boundary layer the velocity in the x-direction is zero.

According to the boundary-layer theory, the pressure change can be neglected along any normal to the surface. A constant pressure difference dp therefore exists between planes 1-1 and 2-2. This pressure difference gives a force on the volume element of magnitude $l \, dp$. In addition to the forces on the surfaces, there is a force due to the weight of the fluid within the volume element

$$\int_0^l \rho g \, dx \, dy$$

Summing up all the forces and equating them to the change in momentum flow gives the momentum equation

$$\frac{d}{dx} \int_0^l (\rho u^2 \, dy) \, dx = l \, dp - \int_0^l \rho g \, dy \, dx - \tau_w \, dx$$

Outside of the boundary layer there is no flow and the pressure difference between planes 1-1 and 2-2 is therefore balanced by the weight of the fluid between the planes

$$dp = \rho_\delta \, g \, dx$$

Multiplying both sides of the last equation by l and changing the right side of the equation to the integral form gives

$$l \, dp = \int_0^l \rho_\delta g \, dx \, dy$$

Introducing the preceding equation into the momentum equation gives

$$\frac{d}{dx}\int_0^l (\rho u^2\, dy)\, dx = g\int_0^l (\rho_\delta - \rho)\, dx\, dy - \tau_w\, dx$$

By introducing the expansion coefficient defined by the equation

$$\beta = \frac{v-v_\delta}{v_\delta}\frac{1}{t-t_\delta}$$

the first term on the right side of the preceding equation can be transformed to

$$g\, dx \int_0^l \beta\rho\, (t-t_\delta)\, dy$$

By designating the difference between the temperature t at the distance y and the temperature t_δ outside of the boundary layer by θ, the following expression is obtained:

$$g\, dx \int_0^l \beta\rho\theta\, dy$$

In the applications considered, the changes in the density and in the expansion coefficient are small compared with their mean values. Therefore, both quantities can be assumed constant in the preceding expressions. The momentum equation for the free-convection boundary layer therefore becomes

$$\frac{d}{dx}\int_0^l u^2\, dy = g\beta\int_0^l \theta\, dy - \frac{\tau_w}{\rho} \qquad (1)$$

A similar equation is set up for the heat flow through the volume element in figure 2. The heat carried with the fluid through plane 1-1 is

$$g \int_0^l \rho c_p u\theta \, dy$$

where the enthalpies $c_p\theta$ are measured from the temperature outside of the boundary layer. The specific heat is considered constant.

The heat carried out of plane 2-2 differs from that carried into plane 1-1 by

$$g \frac{d}{dx}\left(\int_0^l \rho c_p u\theta \, dy \right) dx$$

The difference in the heat flow through planes 1-1 and 2-2 must come from the surface and therefore the heat flow leaving the plate per unit time and area is

$$q_w = g\rho c_p \frac{d}{dx} \int_0^l u\theta \, dy \qquad (2)$$

Equation (2) is the heat-flow equation for the free-convection boundary layer.

Solution of Boundary-Layer Equations

According to von Kármán (reference 5), equations (1) and (2) may be solved by assuming certain shapes for the velocity and temperature profiles within the boundary layer and an empirical relation for the friction force on the wall. By introducing expressions for the velocity and temperature profiles into the preceding momentum and heat-flow equations, the integrations in the equations can be performed. Two total differential equations result, from which two unknown values (for example, the boundary-layer thickness and the maximum velocity within the boundary layer)

can be obtained as functions of x. Naturally, the results of such a calculation are better if the assumed temperature and velocity profiles closely approximate the actual temperature and velocity profiles. It was found, however, that the method is quite insensitive in respect to the shapes assumed. The difficulty in calculating the turbulent free-convection boundary layer in this way is that no information whatsoever exists on the shape of either profile. It is only known that the approximate shapes must be similar to those shown in figure 3. The excess temperature θ has the value θ_w at the wall and decreases steadily towards the value zero, which is reached at a distance δ from the wall. The velocity u has the value zero at the wall and outside of the boundary layer and therefore increases to a maximum value u_{max} with increasing distance from the wall and then decreses again to zero.

The velocity profile in the forced-convection turbulent boundary layer is approximated quite well by the expression

$$u = u_1\left(\frac{y}{\delta}\right)^{1/7} \tag{3}$$

The shape of the velocity profile in the free-convection boundary layer must be different because the velocity is zero outside of the boundary layer as well as on the wall. In the neighborhood of the wall both velocity profiles will probably be similar. Equation (3) is therefore modified by a factor that brings the velocity to zero at the outer border of the boundary layer

$$u = u_1\left(\frac{y}{\delta}\right)^{1/7}\left(1-\frac{y}{\delta}\right) \tag{4}$$

When the maximum velocity is determined by differentiation, it is found that

$$u_1 = 1.54\, u_{max} \tag{5}$$

Equation (4) represents the velocity profile that is used in the first calculation. The profile is shown as $\left(\frac{u}{u_{max}}\right)_I$ in figure 4 together with two other velocity profiles.

In his calculation of the turbulent boundary layer on a rotating disk, von Kármán used the same velocity profile and found good agreement of the calculated friction values with experimental results (reference 5). The calculation of the turbulent free-convection boundary layer is repeated with the other velocity profiles in figure 4 in order to study their effects.

The temperature profile in the turbulent forced-convection flow for Prandtl numbers not too far from 1 is similar to the corresponding velocity profile and it will probably be similar in shape for free-convection flow. The following equation is therefore used for the temperature profile:

$$\theta = \theta_w\left[1-\left(\frac{y}{\delta}\right)^{1/7}\right] \tag{6}$$

The shearing stress τ_w on the wall in turbulent forced-convection flow is given in reference 5 as

$$\tau_w = 0.0225\ \rho u^2\left(\frac{\nu}{uy}\right)^{1/4} \tag{7}$$

By assuming that the same law holds for turbulent free-convection flow in the immediate neighborhood of the wall and considering that the velocity profile (equation (4)) is identical with that represented by equation (3) for very small distances from the wall, equation (7) can be transformed to

$$\tau_w = 0.0225\ \rho u_1^2\left(\frac{\nu}{u_1\delta}\right)^{1/4}$$

By using equation (4) for the velocity distribution, the integral of the first term in the momentum equation (equation 1) is

$$\int_0^l u^2\,dy = u_1^2\delta\int_0^1\left(\frac{y}{\delta}\right)^{2/7}\left(1-\frac{y}{\delta}\right)^2 d\left(\frac{y}{\delta}\right) = 0.207\ u_1^2\delta = 0.491\ u_{max}^2\delta$$

In the preceding equation, the upper limit of the integral was changed from l to $\frac{y}{\delta} = 1$ because equation (4) holds only for $y < \delta$, whereas for $y > \delta$ the velocity is zero.

The integral of the second term in equation (1) is

$$\int_0^l \theta \, dy = \theta_w \delta \int_0^1 \left[1-\left(\frac{y}{\delta}\right)^{1/7}\right] d\left(\frac{y}{\delta}\right) = \frac{1}{8} \theta_w \delta$$

The integral in the heat-flow equation (equation (2)) is

$$\int_0^l u\theta \, dy = u_1 \delta \theta_w \int_0^1 \left(\frac{y}{\delta}\right)^{1/7} \left(1-\frac{y}{\delta}\right)\left[1-\left(\frac{y}{\delta}\right)^{1/7}\right] d\left(\frac{y}{\delta}\right)$$

$$= 0.0681 \, u_1 \theta_w \delta$$

$$= 0.105 \, u_{max} \, \theta_w \delta$$

Substituting the values of the preceding integrals in the momentum and heat-flow equations and considering that the heat-transfer coefficient H can be substituted for the specific heat flow $q_w = H\theta_w$ gives

$$0.491 \frac{d}{dx}\left(u_{max}^2 \delta\right) = \frac{1}{8} g\beta\theta_w \delta - 0.0479 \, u_{max}^2 \left(\frac{\nu}{u_{max}\delta}\right)^{1/4} \qquad (8)$$

$$H = \frac{q_w}{\theta_w} = 0.105 \, g\rho c_p \frac{d}{dx}\left(u_{max}\delta\right) \qquad (9)$$

Solution of equations (8) and (9): Method I. - In order to solve equations (8) and (9), additional information on the heat-transfer coefficient H is necessary. Jakob (reference 4) derived from a compilation of experiments the empirical relation

$$Nu = 0.129 \, (Gr \, Pr)^{1/3} \qquad (10)$$

Because the Nusselt number is proportional to x and the Grashof number is proportional to x^3, the foregoing equation gives a heat-transfer coefficient that is independent of x. With this relation, the differential equation (9) can easily be integrated. Considering the boundary condition that for $x = 0$, $\delta = 0$, the result is

$$u_{max}\delta = \frac{Hx}{0.105\ g\rho c_p} \tag{11}$$

The differential quotient in equation (8) can be transformed by differentiation as follows:

$$\frac{d}{dx}\left(u_{max}^2\delta\right) = u_{max}\frac{d}{dx}\left(u_{max}\delta\right) + u_{max}\delta\frac{du_{max}}{dx}$$

Introducing the values from equations (9) and (11) for the product $u_{max}\delta$ and its differential quotient in equation (8) gives the following differential equation for the velocity u_{max}:

$$\frac{du_{max}}{dx} = 0.254\frac{g\beta\theta_w}{u_{max}} - \frac{u_{max}}{x} - 0.00582\left(\frac{g\rho c_p}{H}\right)^{5/4}\frac{u_{max}^2\nu^{1/4}}{x^{5/4}} \tag{12}$$

No analytical solution was found for this equation, which was therefore solved graphically, as described in appendix B. The results can be approximated with good accuracy by the equation

$$Re_{max} = \frac{u_{max}x}{\nu} = 0.377(Gr\ Pr)^{0.500}\ Pr^{-0.65} \tag{13}$$

Up to now, the boundary-layer thickness has been represented by the value δ, which is the distance from the wall where the velocity (as approximated by equation (4)) and the temperature (according to equation (6)) reach zero values. A more characteristic measure for the boundary-layer thickness in general use is the so-called displacement thickness, which has to be defined for free-convection flow by the equation

$$\delta^* = \int_0^\delta \frac{u}{u_{max}}\,dy$$

which is the thickness the boundary layer would have if the velocity within it were constant and equal to the value u_{max} and the volume flow were the same as in reality.

By using the velocity ratio as determined from equations (4) and (5), the displacement thickness becomes

$$\delta^* = 0.628\ \delta \tag{14}$$

In equation (11) the heat-transfer coefficient H and the maximum velocity u_{max} can be replaced by the Grashof and Prandtl numbers by means of equations (10) and (13). The boundary-layer thickness δ can be changed to the displacement thickness δ^* by means of equation (14), which results in

$$\frac{\delta^*}{x} = 2.04\ (Gr\ Pr)^{-0.167}\ Pr^{-0.35} \tag{15}$$

Solution of equations (8) and (9): Method 2. - Because the graphical solution is a comparatively tedious process, another approach to solve the differential equations (8) and (9) is tried. It will be investigated how closely the equations can be satisfied with the assumption that u_{max} and δ are proportional to some power of the distance x. If

$$u_{max} = C_u x^m \tag{16}$$

and

$$\delta = C_\delta x^n \tag{17}$$

are introduced, equations (8) and (9) become

$$0.491\ C_u^2 C_\delta\ (2m+n) x^{2m+n-1} = \frac{1}{8}\ g\beta\theta_w C_\delta x^n -$$

$$0.0479\ C_u^2 \left(\frac{\nu}{C_u C_\delta}\right)^{1/4} x^{(7/4)m-(1/4)n} \tag{18}$$

and

$$0.105\ g\rho c_p C_u C_\delta\ (m+n)\ x^{m+n-1} = H \tag{19}$$

Inasmuch as these equations must be valid for any value of x, all the exponents of x in any of the equations must be equal. From the momentum equation, values of m and n are obtained:

$$m = 1/2$$

$$n = 7/10$$

It can be seen from the heat-flow equation that the heat-transfer coefficient must be proportional to $x^{1/5}$ in order to fulfill this equation.

By writing

$$H = C_H x^{1/5} \tag{20}$$

and introducing this expression into the heat-flow equation,

$$0.126\ g\rho c_p C_u C_\delta = C_H \tag{21}$$

is obtained. This equation can be solved for

$$C_u = \frac{C_H}{0.126\ g\rho c_p C_\delta} \tag{22}$$

When the value of C_u from equation (22) is introduced into the momentum equation, keeping in mind that $m = 1/2$ and $n = 7/10$, the momentum equation becomes

$$\frac{1}{8} g\beta\theta_w C_\delta^3 - 52.6\left(\frac{C_H}{g\rho c_p}\right)^2 C_\delta - 1.80\left(\frac{C_H}{g\rho c_p}\right)^{7/4} \nu^{1/4} = 0 \tag{23}$$

which is a cubic equation for C_δ that characterizes the boundary-layer thickness.

It is usually assumed that in free-convection flow the Nusselt number is a function of the product of the Grashof and Prandtl numbers. In order to fulfill this condition and equation (20), the Nusselt number for turbulent free-convection flow must be represented by

$$Nu = C(Gr\ Pr)^{2/5} \tag{24}$$

The range of Grashof numbers for which test results are available ($10^{10} < Gr < 10^{12}$) is too small to decide whether equation (10) or (24) is the better one. The test points that are presented in figure 25-3 of reference 4 and figure 129 of reference 7 agree even slightly better with the slope of equation (24). (See fig. 5.) Comparison of this equation with the preceding test results gives for the constant C the numerical value 0.0210. Therefore,

$$Nu = 0.0210\ (Gr\ Pr)^{2/5} \tag{25}$$

If the displacement thickness δ^* is made dimensionless by dividing by a length x and is then introduced into equation (23) together with the dimensionless parameters

$$Gr = \frac{g\beta\theta_w x^3}{\nu^2}$$

$$Pr = \frac{gc_p\mu}{k}$$

$$Nu = \frac{Hx}{k} = 0.0210\ (Gr\ Pr)^{2/5}$$

that characterize the flow and heat transfer in free convection, the following equation is obtained:

$$\left(\frac{\delta^*}{x}\right)^3 - 0.0734\ (Gr\ Pr)^{-0.2}\ Pr^{-1.0}\ \frac{\delta^*}{x} -$$

$$0.00415\ (Gr\ Pr)^{-0.3}\ Pr^{-0.75} = 0 \tag{26}$$

The local heat-transfer coefficient is needed for the calculations presented herein, whereas the test points in fig. 5 are heat-transfer coefficients averaged over the plate length. A slight difference exists between both values; however, inasmuch as the Grashof numbers for the test points are too low to determine the exact numerical value of the constant in equation (24), the constant 0.0210 will be used. Because test results are usually plotted as Nu against (Gr Pr), the product (Gr Pr) was introduced into equation (26).

Equation (26) was numerically solved for several values of (Gr Pr). The results are presented in figures 6 and 7 as $\left(\frac{\delta^*}{x}\right)_I$. Inasmuch as in both logarithmic charts the values for the dimensionless boundary-layer thickness are practically straight lines, the following expression approximates the result of the cubic equation in the indicated range $10^{12} < (\mathrm{Gr\ Pr}) < 10^{15}$ very closely:

$$\frac{\delta^*}{x} = 0.296\ (\mathrm{Gr\ Pr})^{-0.100}\ \mathrm{Pr}^{-0.411} \tag{27}$$

The second unknown value was the maximum velocity within the boundary layer. This value is represented by the Reynolds number

$$\mathrm{Re}_{max} = \frac{u_{max}\, x}{\nu}$$

From equations (16) and (22), u_{max} is determined as a function of C_H. Replacing C_H by means of equations (20) and (25) gives

$$\mathrm{Re}_{max,I} = 0.105\ \frac{\mathrm{Gr}^{2/5}}{\mathrm{Pr}^{3/5}}\left(\frac{x}{\delta^*}\right)$$

By introducing equation (27) for the boundary-layer thickness,

$$\mathrm{Re}_{max,I} = 0.355\ (\mathrm{Gr\ Pr})^{0.500}\ \mathrm{Pr}^{-0.589} \tag{28}$$

is obtained.

In figure 8 the values Re_{max} and δ^*/x, as determined by both methods of solving the differential equations, are compared. It can be seen that the differences are not excessive in the entire range of Grashof numbers investigated, when the lack of information on turbulent free-convection flow is considered; in no case do they exceed 25 percent.

Solutions of Boundary-Layer Equations Using Other Velocity Profiles

The Kármán method used in the preceding section proved comparatively insensitive to the assumed shape of the velocity and temperature profiles in forced-convection flow. In order to check this insensitivity for the free-convection flow, the calculations were repeated using two other expressions for the velocity profiles.

$$u_{II} = u_1 \left(\frac{y}{\delta}\right)^{1/7} \left[1 - \left(\frac{y}{\delta}\right)\right]^2 \tag{29}$$

$$u_1 = 1.69\, u_{max}$$

$$u_{III} = u_1 \left(\frac{y}{\delta}\right)^{1/7} \left[1 - \left(\frac{y}{\delta}\right)^{1/4}\right] \tag{30}$$

$$u_1 = 2.80\, u_{max}$$

The shapes of these velocity profiles, together with the first assumption and the temperature profile, are shown in figure 4. The calculations resulted in the following equations:

$$\left(\frac{\delta^*}{x}\right)^3_{II} - 0.0315\, (Gr\, Pr)^{-0.2}\, Pr^{-1.0} \left(\frac{\delta^*}{x}\right)_{II} -$$

$$0.00218\, (Gr\, Pr)^{-0.3}\, Pr^{-0.75} = 0 \tag{31}$$

$$\left(\frac{\delta^*}{x}\right)_{III}^3 - 0.0308\ (Gr\ Pr)^{-0.2}\ Pr^{-1.0} \left(\frac{\delta^*}{x}\right)_{III} -$$

$$0.00583\ (Gr\ Pr)^{-0.3}\ Pr^{-0.75} = 0 \qquad (32)$$

For the dimensionless displacement thickness of the boundary layer, the equations can be approximated in the range of Grashof numbers from 10^{10} to 10^{15} by

$$\left(\frac{\delta^*}{x}\right)_{II} = 0.205\ (Gr\ Pr)^{-0.100}\ Pr^{-0.358} \qquad (33)$$

$$\left(\frac{\delta^*}{x}\right)_{III} = 0.235\ (Gr\ Pr)^{-0.100}\ Pr^{-0.328} \qquad (34)$$

The Reynolds numbers characterizing the maximum velocities can be approximated by

$$Re_{max,II} = 0.418\ (Gr\ Pr)^{0.500}\ Pr^{-0.642} \qquad (35)$$

$$Re_{max,III} = 0.384\ (Gr\ Pr)^{0.500}\ Pr^{-0.672} \qquad (36)$$

Discussion of Results

The boundary-layer thicknesses and the maximum Reynolds numbers, as determined with the three velocity profiles, differ only in the constant and slightly in the exponent of the Prandtl number. The average value of the constant for the boundary-layer thickness, based on the three values that were obtained with the different velocity profiles, is 0.245 and the three individual constants deviate by ±20 percent from this average value. The corresponding average for the constant in Re_{max} is 0.386 and the individual

values deviate by ±8 percent from this average value. So it can be seen that the influence of the shape of the assumed profiles is not large. Of course, there may be an additional deviation of the calculated values from the real ones, which is caused by the uncertainty of the value for the shearing stresses. The calculations can be improved in this direction as soon as more information on this value in turbulent free-convection flow is available.

It is quite interesting to see by which factors the coefficients m and n in equations (16) and (17) are influenced. A check of the calculations leading to these equations shows that the value $m = 1/2$ follows from the assumption that the boundary-layer thickness and the maximum velocity increase with some power of x. The same value for the coefficient m is valid in the laminar range. The value for the coefficient n also depends on the law for the shearing stress τ_w. A value of n may be determined by assuming that the heat-transfer coefficient is independent of x.

The calculation in this manner gives the result that the shearing stress τ_w has to depend on the power $-1/2$ of the Reynolds number uy/ν in order to fulfill this demand. This large deviation from the law for the shearing stress in forced-convection turbulent flow (equation (7)), where the corresponding power is $-1/4$, seems improbable. The shape of the velocity or temperature profile does not influence m or n.

Another assumption involved in the calculations should be mentioned. In assuming that the boundary-layer thickness δ is proportional to x^m, it is implied that the turbulent boundary layer begins with the thickness zero at the lower end of the plate. In reality, first a laminar boundary layer occurs and then the turbulent boundary layer develops within a certain distance x out of the laminar boundary layer. The same assumption that is made here is ordinarily used for calculating the turbulent boundary layer for forced flow along a plate and proves quite successful (reference 8). In addition, the relative range of the laminar boundary layer at the high Grashof numbers encountered in turbine operation is so small that an error in the correct starting point of the turbulent boundary layer influences the result of the calculations to a very small degree.

Comparison with Experiments

A one-stage gas turbine with liquid free-convection cooling was tested at the NACA Lewis laboratory (reference 9). The results of these tests may be used to make a first check on the calculations. The tested turbine wheel had a mean radius r_m of 5.72 inches. Each blade of the wheel had five holes with a length L of 2.5 inches. Three holes were 0.125 inch in diameter, one was 0.090, and one was 0.060 inch in diameter. The circumferential velocity of the blades at the mean radius was approximately 700 feet per second. This velocity gives 1,030,000 feet per second per second for the centrifugal acceleration. This high acceleration, which is 32,000 times the acceleration due to gravity, explains the large Grashof numbers attained in these holes. The cooling water had a temperature of approximately 110° F. The blade-wall temperature was 425° F. By using the preceding values and a film temperature of 200° F for the property values, the Grashof number is found to be 1.25×10^{14}. Considering the Prandtl number to be 1.74, the Grashof number to be 1.25×10^{14}, and the kinematic viscosity to be 3.16×10^{-6} square feet per second, introducing these values into equations (27) and (28), and solving for δ^* and u_{max} gives $\delta^* = 0.0214$ inch and $u_{max} = 58$ feet per second. If the diameter of a cooling hole is determined in such a way that the water velocity has the same value in the core of the fluid as in the heated boundary layer, the value for this diameter is found to be 0.146 inch. In a hole of such a diameter, the heat-transfer coefficient has surely already decreased as compared with a big-diameter hole. A comparison of this value with the diameters of the holes that were used in the test turbine leads to the conclusion that the circulation of the cooling water in these holes must have been quite restricted.

In the tests, the average heat-transfer coefficient for all holes was measured. The corresponding Nusselt numbers are plotted in figure 5. The same figure shows the Nusselt numbers calculated with equation (24) and with equation (10) given by Jakob. Both Nusselt numbers refer to the heat-transfer coefficient in a hole with a large diameter. Some test results are also shown in figure 5. They were taken from figure 25-3 of reference 4 and figure 129 of reference 7. It can be seen that equation (24) and Jakob's equation fit the test results equally well and that the Nusselt values given by both equations are very much larger than the Nusselt numbers measured in the test turbine; so the conclusion, which is drawn from the calculations, that the holes in the test turbine were too small in diameter for proper circulation, is confirmed.

Inasmuch as it is impossible to avoid holes with small diameters in turbine blades, the question arises as to how the circulation can be improved in these holes. This problem will be dealt with in the following section.

A brief calculation reveals that vaporization will never occur in a hole if its diameter is large enough for good circulation. By using equation (25), (Gr Pr) equal to 10^{14}, and a thermal conductivity of 0.393 (Btu/(hr)(ft)(°F)), the heat-transfer coefficient in the hole was found to be 15,500 (Btu/(hr)(sq ft)(°F)). The heat-transfer coefficient on the outside of the blade is usually in the neighborhood of 80 (Btu/(hr)(sq ft)(°F)). These values determine the temperature difference θ_w between the wall (or the hottest portion in the fluid) and the fluid entering the hole. By using the preceding values, it is found that for a large hole θ_w is equal to 9.1° F. Evaporation occurs when the wall temperature reaches or exceeds the saturation temperature of the water. In the holes a considerable pressure increase occurs with increasing distance from the axis of rotation. This increase can easily be calculated from a balance between the pressure and centrifugal forces. The saturation temperature rises with the pressure and it is found that an increase in radius of only 0.004 inch is sufficient to increase the saturation temperature by 9.1° F. Therefore, even if the liquid enters the holes in a saturated state, evaporation will occur only at the entrance.

With the reduced circulation in the experimental turbine and the corresponding decrease in heat-transfer coefficient in the holes, conditions are greatly changed and evaporation may occur in the inner part of the holes.

The velocities connected with the free-convection flow are extremely high when the holes are large enough in diameter, which results in very high heat-transfer coefficients and is a definite advantage of the free-convection cooling as compared with forced-convection cooling. With the forced-convection method it is ordinarily impossible to obtain equally high velocities.

FREE-CONVECTION HEAT TRANSFER IN LOOP

Turbulent Flow

The circulation in the holes with small diameters decreases because the boundary layer does not leave enough space through which the cold liquid may enter the holes in a direction opposite the flow

in the boundary layer. It is therefore to be expected that the circulation in the holes can be materially improved when the cold fluid is fed into the holes from the top of the blade (fig. 9). In the central part of turbine blades, it is always possible to provide holes with larger diameters. If a connection is made on top of the blade between these larger holes and the small holes in the leading and trailing edges of the blade, cold liquid will flow from the large-diameter holes to the small holes. The proposed arrangement of cooling passages in free-convection liquid-cooled turbine blades in shown in figure 10.

In order to see how much the heat transfer in a small hole can be improved in this manner, a calculation is made as follows: Hole (1) (fig. 9), with a very small diameter, is connected on top with a second hole (2) of very large diameter. The diameter of hole (1) may be so small that the boundary layers fill out the whole cross section and the liquid flows only in a downward direction. The velocity profile will then have practically the same shape as in forced-convection flow. The same thing will be true for the value of the friction forces. The calculations using the friction factor and heat-transfer coefficient of forced flow in a tube are therefore applicable. First, the change of the bulk temperature t of the liquid along the hole may be calculated. For this purpose, a heat balance is set up for the length dx of the tube, assuming the temperature t_w of the tube wall to be constant along the whole length. Denoting the average velocity in the hole by U and the heat-transfer coefficient built with the local temperature difference t_w-t_b by H_b yields

$$c_p g\rho U \frac{\pi D^2}{4} dt_b = H_b \pi D(t_w-t_b)\, dx \tag{37}$$

By introducing the difference θ_b between the temperature of the wall and the bulk temperature of the liquid and the difference between the temperature of the wall and the cold liquid entering the hole $\theta_w = t_w-t_0$, equation (37) transforms into

$$\frac{d\theta_b}{\theta_b} = \frac{-4H_b}{c_p g\rho DU} dx \tag{38}$$

Integration with the condition that for $x = 0$, $\theta_b = \theta_w$ leads to the expression

$$\theta_b = \theta_w e^{-\frac{4H_b x}{gc_p \rho DU}}$$

and for the temperature difference at the exit of the hole $(x = L)$,

$$\theta_{b,e} = \theta_w e^{-\frac{4H_b L}{gc_p \rho DU}}$$

The logarithmic mean temperature difference that is to be used for heat-transfer calculations is

$$\theta_m = \frac{\theta_{b,e} - \theta_w}{\log_e \frac{\theta_{b,e}}{\theta_w}}$$

Introducing the preceding values gives

$$\frac{\theta_m}{\theta_w} = \frac{c_p g \rho \, DU}{4H_b L}\left(1 - e^{-\frac{4H_b L}{gc_p \rho DU}}\right) \tag{39}$$

The force that generates the movement of the liquid through the loop is the sum of all the buoyancy forces. The pressure difference connected with these buoyancy forces along the length dx is

$$dp = g(\rho_\delta - \rho_b)\, dx$$

Introducing the expansion coefficient in the same way as was previously done and assuming the changes in specific weight to be small gives

$$dp = g\rho_\delta \beta(t_b - t_\delta)\, dx = g\rho_\delta \beta(\theta_w - \theta_b)\, dx$$

The pressure difference available to overcome the friction in the small-diameter hole is

$$\Delta p = \int_0^L dp = g\rho_s \beta \theta_w \left[L - \frac{c_p g \rho D U}{4H_b} \left(1 - e^{-\frac{4H_b L}{g c_p \rho D U}} \right) \right] \tag{40}$$

This pressure difference is used up by the friction forces. It is assumed that the flow is turbulent in the small-diameter hole and that the formula for pressure drop for turbulent forced-convection flow as given in reference 4 (p. 433) can be used:

$$\Delta p = 0.316 \frac{1}{Re_D^{1/4}} \rho \frac{U^2}{2} \frac{L}{D} \tag{41}$$

Introducing this expression into equation (40) and converting into dimensionless values gives

$$0.158 \frac{Re_D^{1.75}}{Gr \left(\frac{D}{L} \right)^3} = 1 - \frac{Re_D Pr}{4 Nu_b} \frac{D}{L} \left(1 - e^{-\frac{4 Nu_b}{Re_D Pr} \frac{L}{D}} \right) \tag{42}$$

where $Nu_b = HD/k$. The expression on the right side of the equation can be simplified because it turns out, in the range of Grashof numbers of 10^{13} to 10^{15} and of length-diameter ratios less than 50, that the exponent of e is a small value. The expression on the right side of equation (42) has the form $1 - 1/z(1-e^{-z})$. Transforming the e function into a series and considering only the first three terms gives

$$1 - \frac{1}{z} \left[1 - \left(1 - z + \frac{z^2}{2} \right) \right] = \frac{z}{2} \tag{43}$$

The Nusselt number for forced-convection turbulent flow in a tube is given in reference 7 (p. 168) as

$$Nu_b = 0.023 Re_D^{0.8} Pr^{0.4} \tag{44}$$

Therefore, equation (42) simplifies to

$$\frac{Re_D^{1.75}}{Gr\left(\frac{D}{L}\right)^3} = \frac{12.66\ Nu_b}{Re_D Pr}\frac{L}{D} = \frac{0.291}{Re_D^{0.2} Pr^{0.6}}\frac{L}{D} \tag{45}$$

which may be solved for the Reynolds number

$$Re_D = \frac{0.531\ Gr^{0.513}}{Pr^{0.308}}\left(\frac{D}{L}\right)^{1.03} \tag{46}$$

In equation (44), the Nusselt number and the Reynolds number are based on the diameter of the tube and the heat-transfer coefficient H_b with the mean difference between the wall and the liquid bulk temperature. In the previous calculations, the length x and the difference θ_w between the wall temperature and the temperature of the entering cold liquid was used as a basis for the heat-transfer coefficient and the Nusselt number. In order to make possible a comparison of Nusselt numbers, equation (44) is converted to this Nusselt number. The specific heat flow q_w from the wall into the liquid must be the same expressed by both heat-transfer coefficients. Therefore

$$H_b\theta_m = H\theta_w$$

Inasmuch as the calculations here are for the whole tube length ($x = L$), the Nusselt number Nu used in previous calculations is connected with the Nusselt number Nu_b, based on the diameter and the mean temperature difference, by

$$Nu = Nu_b \frac{L}{D}\frac{\theta_m}{\theta_w} \tag{47}$$

Introducing the values for the mean temperature difference θ_m from equation (39), the values for Nu_b from equation (44), and simplifying according to equation (43) gives

$$Nu = 0.023\ Re_D^{0.8}\ Pr^{0.4}\ \frac{L}{D}\left(1 - \frac{0.046}{Re_D^{0.2} Pr^{0.6}}\ \frac{L}{D}\right) \tag{48}$$

The Reynolds number may be inserted from equation (46),

$$Nu = 0.0139\ Gr^{0.41}\ Pr^{0.154}\left(\frac{L}{D}\right)^{0.176}\left[1 - \frac{0.0522}{Gr^{0.103}\ Pr^{0.538}}\left(\frac{L}{D}\right)^{1.21}\right] \tag{49}$$

Laminar Flow

When the Reynolds number is smaller than the critical value of 2100 (reference 7, p. 154), the flow in the small-diameter hole is laminar. In this case, the following formulas for the pressure drop and heat-transfer coefficient in laminar forced flow are used:

$$\left.\begin{aligned} \Delta p &= 32\ \frac{\mu U L}{D^2} \\ Nu_b &= \frac{HD}{k} = 3.65 \end{aligned}\right\} \tag{50}$$

The formula for the Nusselt number (reference 4, p. 530) is derived from calculations by Nusselt and is valid only for fully developed flow. In the inflow region, higher values occur and another more complicated formula has to be used. Because the simple formula (50) gives minimum values, it is used here. Carrying out the calculations in the same manner as for turbulent flow results in

$$\frac{32\ Re_D}{Gr}\left(\frac{L}{D}\right)^3 = \left[1 - \frac{Re_D Pr}{14.6}\ \frac{D}{L}\left(1 - e^{-\frac{14.6}{Re_D Pr}\ \frac{L}{D}}\right)\right] \tag{51}$$

$$Nu = 3.65\left(\frac{L}{D}\right)\left[1 - 32\ \frac{Re_D}{Gr}\left(\frac{L}{D}\right)^3\right] \tag{52}$$

Discussion of Results

The Nusselt numbers were calculated from equation (49) for a loop, the small hole of which has ratios $L/D = 25$ and 50. The results are shown in figure 5. With equation (46), it was ascertained that in the range shown in figure 5 the flow is turbulent. The minimum Reynolds number calculated was 20,000. It can be seen that very high Nusselt numbers are obtained in this way. The Nusselt numbers are even larger than in a hole closed on top with very large diameter-to-length ratio.

The large heat-transfer coefficients obtained by means of the loop can be used in turbine-blade design, a fact that will be discussed in the last section of the report.

ACTION OF CORIOLIS FORCES

Up to now the action of the Coriolis forces on the flow of the cooling liquid in the holes has been neglected. In order to get an estimate of the effect of these forces on the flow and the heat transfer, the magnitude of these forces is compared with the centrifugal forces. In the holes the relative movement of the fluid is normal to the circumferential velocity of the blade. In this case, the Coriolis acceleration is

$$2u\omega \tag{53}$$

The acceleration has the same direction as the circumferential velocity when the relative velocity points toward the axis of rotation. When the relative velocity is directed away from the axis of rotation, the Coriolis acceleration acts in a direction opposite to the circumferential velocity. The comparison with the centrifugal forces will be made in the cross section of the hole fixed by the mean radius r_m. In a cross section of the hole, the relative velocities of the fluid vary between zero and the maximum value as previously indicated. The greatest difference between the Coriolis acceleration acting on different fluid particles in the cross section therefore has the value

$$2u_{max}\omega$$

This acceleration is compared with the acceleration connected with the buoyancy forces:

$$r_m \omega^2 \beta \theta$$

The maximum difference in the temperature difference in one cross section is θ_w. Therefore, the maximum buoyant acceleration due to the centrifugal force is

$$r_m \omega^2 \beta \theta_w$$

The ratio ζ of the maximum Coriolis acceleration to the maximum acceleration connected with the buoyant forces is

$$\zeta = \frac{2u_{max}}{r_m \omega \beta \theta_w} \tag{54}$$

The velocity u_{max} may be expressed by the corresponding Reynolds number Re_{max}. Expressing, in addition, the angular velocity ω by the Grashof number $r_m \omega^2 \beta \theta_w x^3 / \nu^2$, which has to be used for convection caused by centrifugal fields, gives

$$\zeta = 2\ Re_{max} \frac{1}{Gr^{0.5}} \left(\frac{x/r_m}{\beta \theta_w} \right)^{0.5} \tag{55}$$

Inserting the Reynolds number from equation (28) yields

$$\zeta = 0.71 \frac{1}{Pr^{0.089}} \left(\frac{x/r_m}{\beta \theta_w} \right)^{0.5} \tag{56}$$

At the mean radius r_m, x is equal to $L/2$. The ratio x/r_m has values near 1/4. In the tests on the free-convection liquid-cooled turbine, the highest value of the temperature difference θ was 315° F. The film temperature for evaluating property values of the cooling water was 200° F. When this film temperature is used, the Prandtl number is 1.74 and the expansion coefficient 0.00043/° F. Inserting these values into equation (56) gives the value 0.84 for the ratio of the Coriolis acceleration to the acceleration connected with the buoyancy forces in the cross section of the hole. The Coriolis forces are therefore quite appreciable.

The Coriolis forces set up a secondary movement of the type shown in figure 11. The secondary flow is similar to the one in a bent tube. It increases the boundary-layer thickness on the side of the hole in the direction of the rotation and decreases its thickness on the opposite side.

To some extent it is possible to study the influence of this secondary movement on heat transfer by means of static tests previously described. By inclining the static test section, the free-convection-flow setup would be exactly similar to the flow in the rotating hole in the turbine blade if the velocity and temperature profiles would be similar. In reality, the profiles differ in shape; however, the comparison may be used as a first estimate of the Coriolis forces. The ratio of Coriolis to centrifugal acceleration of 1.00 corresponds to a static tube inclined at 45° from the vertical. Unfortunately, no test results are known for gravitational free-convection flow in an inclined heated tube. Measurements were made, however, on gravitational free-convection flow in an air layer between two parallel plates, vertical and inclined, and in an air layer between two coaxial cylinders. In both cases it was found that the heat-transfer coefficient changed very little when the test setup was inclined from the vertical position to an angle of 45°; the change was about 20 percent (reference 4). This information gives some indication that even when the ratio of the Coriolis to the centrifugal forces is considerable, the ratio does not affect the heat transfer to a large degree.

SUMMARIZING REMARKS AND RECOMMENDATIONS

The method of free-convection cooling of rotating turbine blades utilizes the intense currents generated in the liquid, which fills the hollow spaces within the blades, by the centrifugal forces as soon as temperature differences are present in the liquid. In the current designs using this method, holes are provided within the blades that are closed on top and connected with some liquid supply at the blade root. Such a blade was shown and the free-convection currents set up in one hole of the blade were illustrated. The heated fluid within the boundary layer along the wall of the hole moves toward the blade root and is replaced by cold liquid flowing toward the top in the central part of the hole. When the diameter of the hole is very small as compared with the length, the two liquid streams flowing in opposite directions hinder each other and the circulation and cooling effect decrease. A measure of this limiting diameter-to-length ratio was obtained by calculating the boundary-layer thickness of the free-convection flow in a hole with a very large diameter-to-length ratio.

Inasmuch as the flow in the boundary layer is turbulent under the conditions present in a rotating turbine blade, the approximate method introduced by von Kármán was used for the calculations. In this method the shapes of the velocity and temperature profiles have to be assumed. Unfortunately, no information is available on the shape of either profile in turbulent free-convection flow. The calculations were therefore carried through with three different shapes for the velocity profile. The shape of the temperature profile was assumed to be identical to the one in turbulent forced-convection flow. Also, the law for the shearing stress on the wall in forced flow was used. The method proved quite insensitive to a change in the shape of the profiles. The values of the boundary-layer thickness and of the maximum velocity for the flow in the range covered by the results of the calculations with the different assumptions varied approximately 20 percent. A more accurate answer to the problem can be obtained only when more experimental information is available on the shapes of the profiles.

The calculations and their comparison with test results on a free-convection cooled turbine indicated that in blades of 2.5-inch length the circulation and the cooling effect are decreased to a considerable degree in holes with diameters less than 0.146 inch. The circulation and heat removal of a hole with a small diameter-to-length ratio can, however, be restored to the value of one with a large diameter-to-length ratio when the hole with the small diameter-to-length ratio is connected on top of the blade with neighboring large-diameter-to-length-ratio holes. A second set of calculations proved this fact.

From the calculations, the following recommendations for the arrangement of the cooling holes in turbine blades can be made. The blade should be thick in the central part so that holes with large diameters can be arranged there. These holes should be connected on top of the blade with the small-diameter holes. Such an arrangement of cooling holes in a turbine blade was shown. For especially effective cooling, the cross section of the holes should be as large as possible. It must be kept in mind, of course, that very high pressures are present inside the holes and that the walls must withstand these pressures. The stresses caused by the internal pressures in the holes must be added to the stresses caused by the centrifugal forces in the solid material of the blades.

In the boundary-layer calculation, the effect of the Coriolis forces on the movement of the liquid in the rotating holes was neglected. Experiments on gravitational free-convection flow on inclined objects indicated that this effect is of little importance on the heat transfer.

Lewis Flight Propulsion Laboratory,
National Advisory Committee for Aeronautics,
Cleveland, Ohio.

APPENDIX A

SYMBOLS

The following symbols are used in this report:

C	constant
C_H	constant for variation of heat-transfer coefficient with $x^{1/5}$
C_u	constant for variation of maximum velocity in boundary layer with x^m
C_δ	constant for variation of boundary-layer thickness with x^n
c_p	specific heat at constant pressure, Btu/(lb)(°F)
D	diameter, ft
Gr	Grashof number, $\frac{g\beta\theta_w x^3}{\nu^2}$
g	acceleration due to gravity, ft/sec^2
H	heat-transfer coefficient, Btu/(sq ft)(sec)(°F)
k	heat conductivity, Btu/(ft)(sec)(°F)
L	length of hole, ft
l	length, ft, (fig. 2)
m	exponent
Nu	Nusselt number, $\frac{Hx}{k}$
n	exponent
Pr	Prandtl number, $\frac{\nu}{\alpha} = \frac{gc_p\mu}{k}$
p	pressure, lb/sq ft
q	specific heat flow, Btu/(hr)(sq ft)
Re_D	Reynolds number based on diameter D, $\frac{UD}{\nu}$

Re_{max} Reynolds number based on maximum velocity u_{max}, $\frac{u_{max}\, x}{\nu}$

r radius, ft

t temperature, °F

U velocity, ft/sec

u velocity component in x-direction, ft/sec

u_1 velocity outside boundary layer of comparable forced-convection flow, ft/sec

v specific volume, cu ft/lb

x coordinate (distance from starting point of boundary layer), ft

y coordinate (distance from wall), ft

α thermal diffusitivity, sq ft/sec

β expansion coefficient, 1/°F

δ boundary-layer thickness, ft

δ^* displacement thickness of boundary layer, ft

ζ ratio of maximum Coriolis acceleration to maximum centrifugal acceleration

θ temperature difference, °F

θ_w temperature difference between wall and fluid outside of boundary-layer, °F

μ dynamic viscosity, (lb)(sec)/sq ft

ν kinematic viscosity, sq ft/sec

ρ dynamic density, $(lb)(sec^2)/ft^4$

τ shearing stress, lb/sq ft

ω angular velocity, 1/sec

Subscripts:

b bulk value (mixed mean)

e	exit condition
m	mean value
max	maximum value
w	on wall
δ	on outer border (and outside) boundary layer
I	values calculated with first assumption for velocity profile
II	values calculated with second assumption for velocity profile
III	values calculated with third assumption for velocity profile

APPENDIX B

SOLUTION OF EQUATION (12)

The differential equation to be solved is

$$\frac{du_{max}}{dx} = 0.254 \frac{g\beta\theta_w}{u_{max}} - \frac{u_{max}}{x} - 0.00582 \left(\frac{g\rho c_p}{H}\right)^{5/4} \frac{u_{max}^2 \nu^{1/4}}{x^{5/4}} \quad (12)$$

It is advantageous to transform this equation by the use of non-dimensional values. The Grashof number Gr is used to replace the independent variable x and the Reynolds number $Re_{max} = \frac{u_{max} x}{\nu}$ for the dependent variable u_{max}. Differentiating the Reynolds number gives

$$\frac{d(Re_{max})}{dx} = \frac{x}{\nu} \frac{du_{max}}{dx} + \frac{u_{max}}{\nu} \quad (57)$$

Introducing the differential quotient du_{max}/dx from this expression, and the Grashof number into equation (12) yields

$$\frac{d(Re_{max})}{d(Gr)} = \frac{0.0852}{Re_{max}} - \frac{0.00194\ Re_{max}^2\ Pr^{5/4}}{Gr\ Nu^{5/4}}$$

The Nusselt number is replaced by use of equation (10), which gives

$$\frac{d(Re_{max})}{d(Gr)} = \frac{0.0852}{Re_{max}} - \frac{0.0250\ Re_{max}^2\ Pr^{5/6}}{Gr^{17/12}} \quad (58)$$

This equation was graphically solved (fig. 12). Inasmuch as the range of Grashof numbers concerned is fairly wide, it is advantageous to obtain the graphical solution in a logarithmic diagram in which the Reynolds number is plotted over the Grashof number on a logarithmic scale. In order to determine the curves that present the solution of the differential equation in the diagram, the slope for any pair of values Re and Gr is needed. If $\log_e Re_{max} = \psi$ and $\log_e Gr = \xi$, then the needed slope is

$$\frac{d\psi}{d\xi} = \frac{Gr}{Re_{max}} \frac{d(Re_{max})}{d(Gr)} \tag{59}$$

For any pair of values Re_{max} and Gr, the differential quotient $\frac{d(Re_{max})}{d(Gr)}$ can be determined from equation (58). Equation (59) gives the slope in the logarithmic plot. Figure 12 shows the slopes determined in this way for two Prandtl numbers. The needed solution of the differential equation (58) must fulfill the condition that for $Gr = 0$, $Re_{max} = 0$. This condition follows from the assumption that the turbulent boundary layer starts with a thickness zero at x equal to zero. The validity of this assumption was previously discussed. In starting out with high Grashof numbers and drawing curves that have the described slopes for all Grashof numbers, it is found that the curve that fulfills the preceding condition can be found with very good accuracy. All curves that start out with a Reynolds number that is too great turn away in an upward direction as the Grashof number is decreased. Curves that start out at high Grashof numbers with a low Reynolds number turn away in a downward direction.

REFERENCES

1. Schmidt, E.: The Possibilities of the Gas Turbine for Aircraft Engines. Reps. & Trans. No. 489, GDC 2504 T, British M.O.S.

2. Schmidt, Ernst, und Beckmann, Wilhelm: Das Temperatur- und Geschwindigkeitsfeld vor einer Wärme abgebenden senkrechten Platte bei natürlicher Konvektion. Tech. Mech. Thermodynam., Bd. 1, Heft 10 und 11, 1930, S. 1-24.

3. Saunders, O. A.: The Effect of Pressure upon Natural Convection in Air. Proc. Roy. Soc. London, vol. 157, no. A891, ser A, Nov. 2, 1936, pp. 278-291.

4. Jakob, Max: Heat Transfer, vol. I. John Wiley & Sons, Inc., 1949.

5. von Kármán, Th.: On Laminar and Turbulent Friction. NACA TM 1092, 1946.

6. Goldstein, Sidney: Modern Developments in Fluid Dynamics, vol. II. Clarendon Press (Oxford), 1938, p. 641.

7. McAdams, William H.: Heat Transmission. McGraw-Hill Book Co., Inc., 2d ed., 1942.

8. Anon.: Ergebnisse der aerodynamischen Versuchsanstalt zu Gottingen, Herausgegeben L. Prandtl und A. Betz. Lieferung III. R. Oldenbourg (Berlin), 1927, p.4.

9. Freche, John C., and Diaguila, A. J.: Heat-Transfer and Operating Characteristics of Aluminum Forced-Convection and Stainless-Steel Natural-Convection Water-Cooled Single-Stage Turbines. NACA RM E50D03a, 1950.

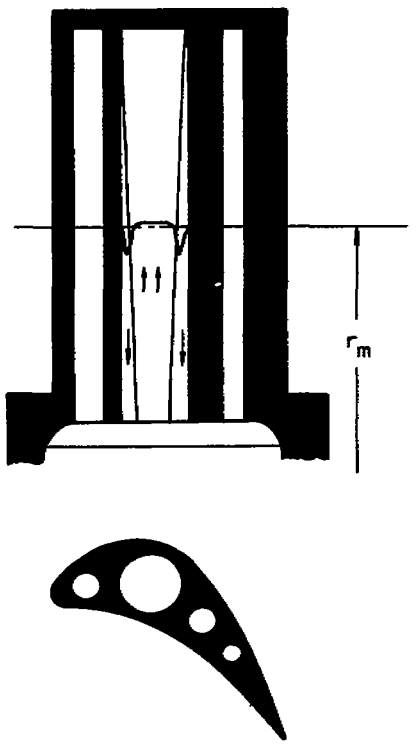

Figure 1. - Free-convection liquid-cooled turbine blade.

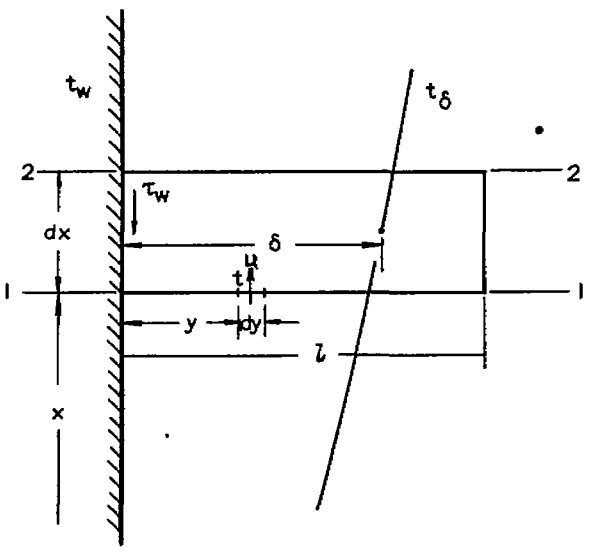

Figure 2. - Nomenclature in deriving equations for free-convection boundary layer.

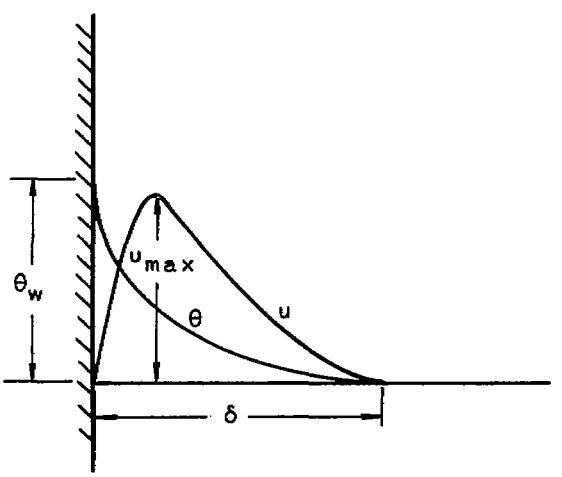

Figure 3. - Shape of temperature and velocity profiles in turbulent free-convection boundary layer.

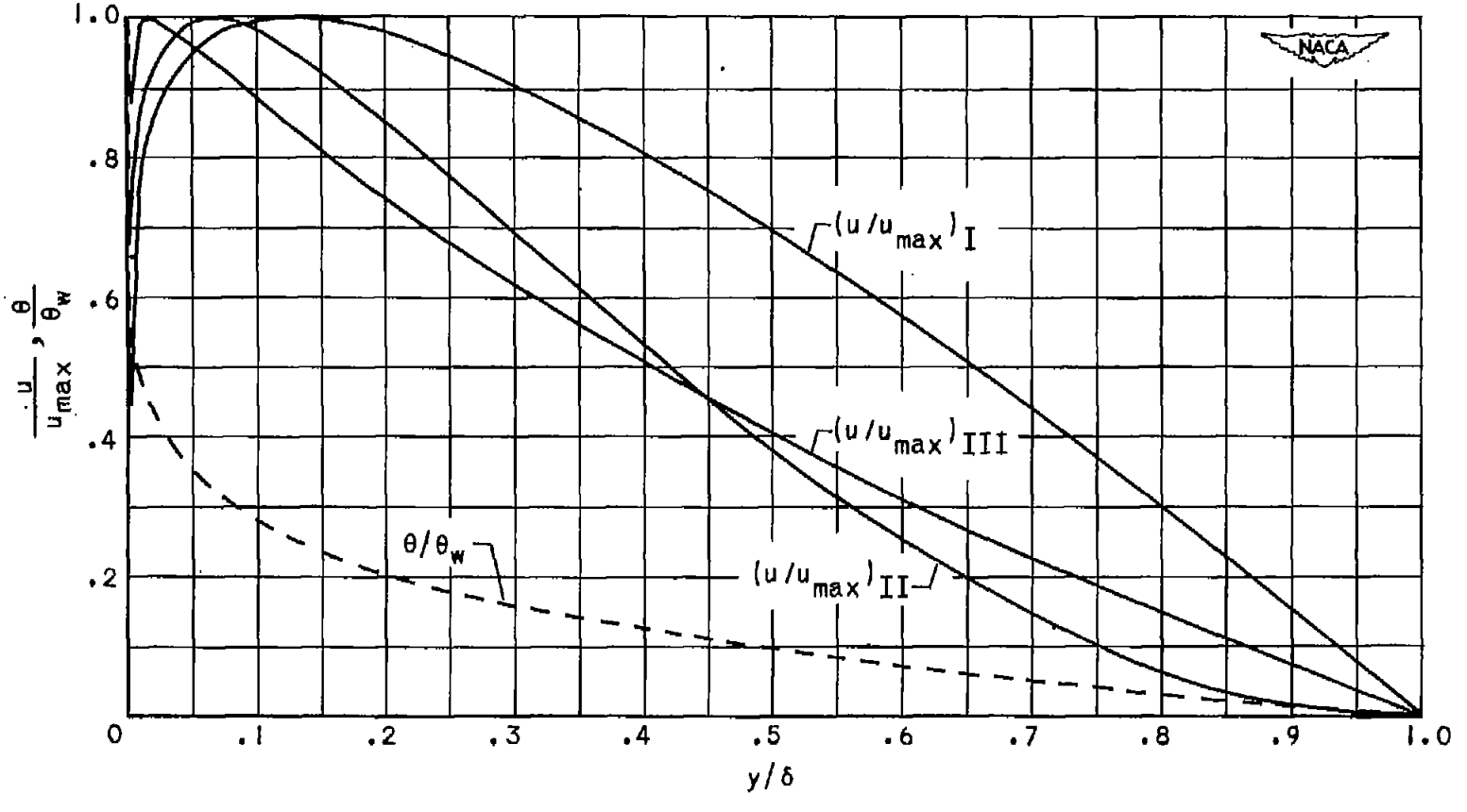

Figure 4. – Assumed velocity profiles and temperature profile for boundary-layer calculations.

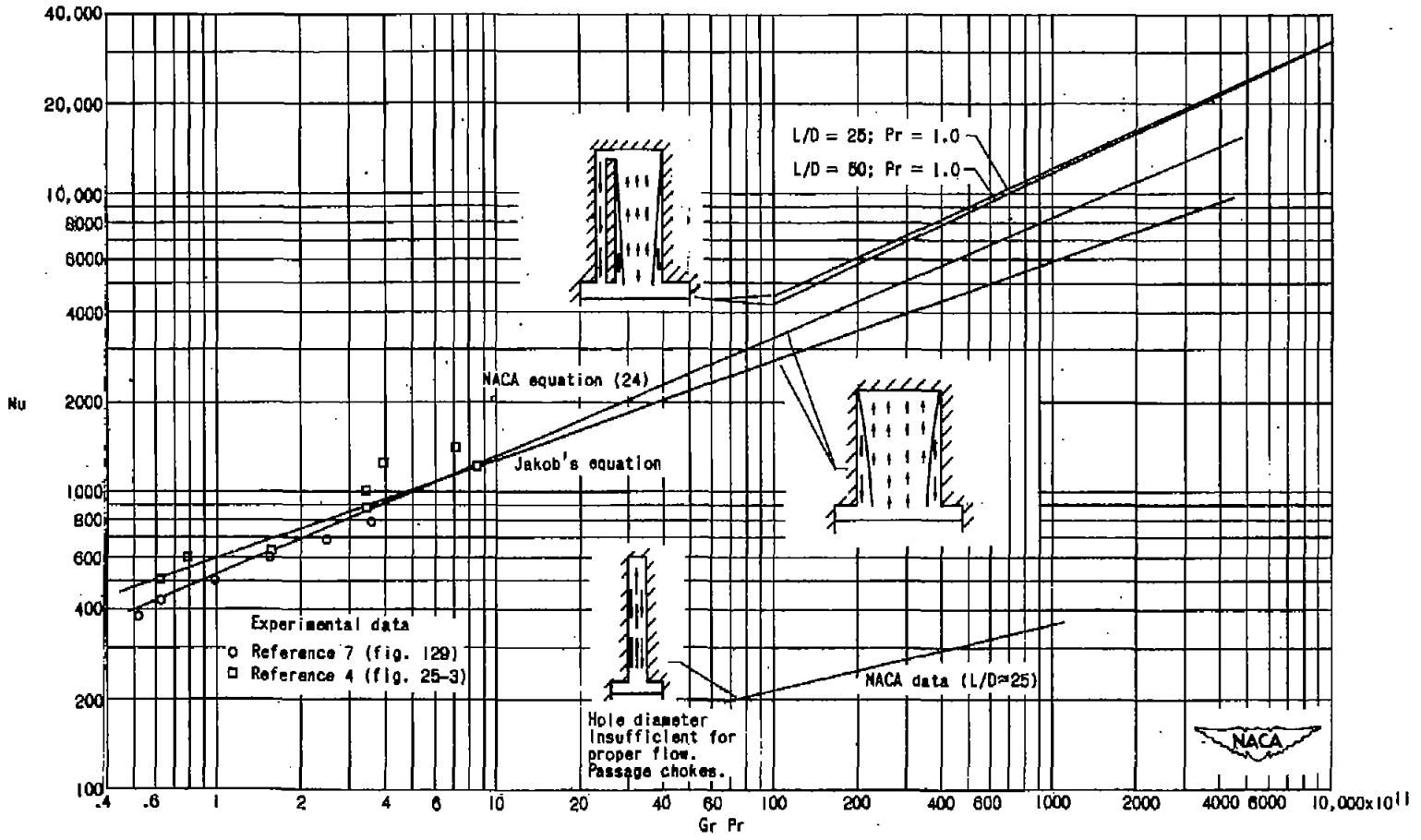

Figure 6. - Comparison of Nusselt numbers measured on free-convection liquid-cooled turbine, calculated for closed hole with large diameter-length ratio and for hole of small diameter-length ratio connected to hole of large diameter-length ratio.

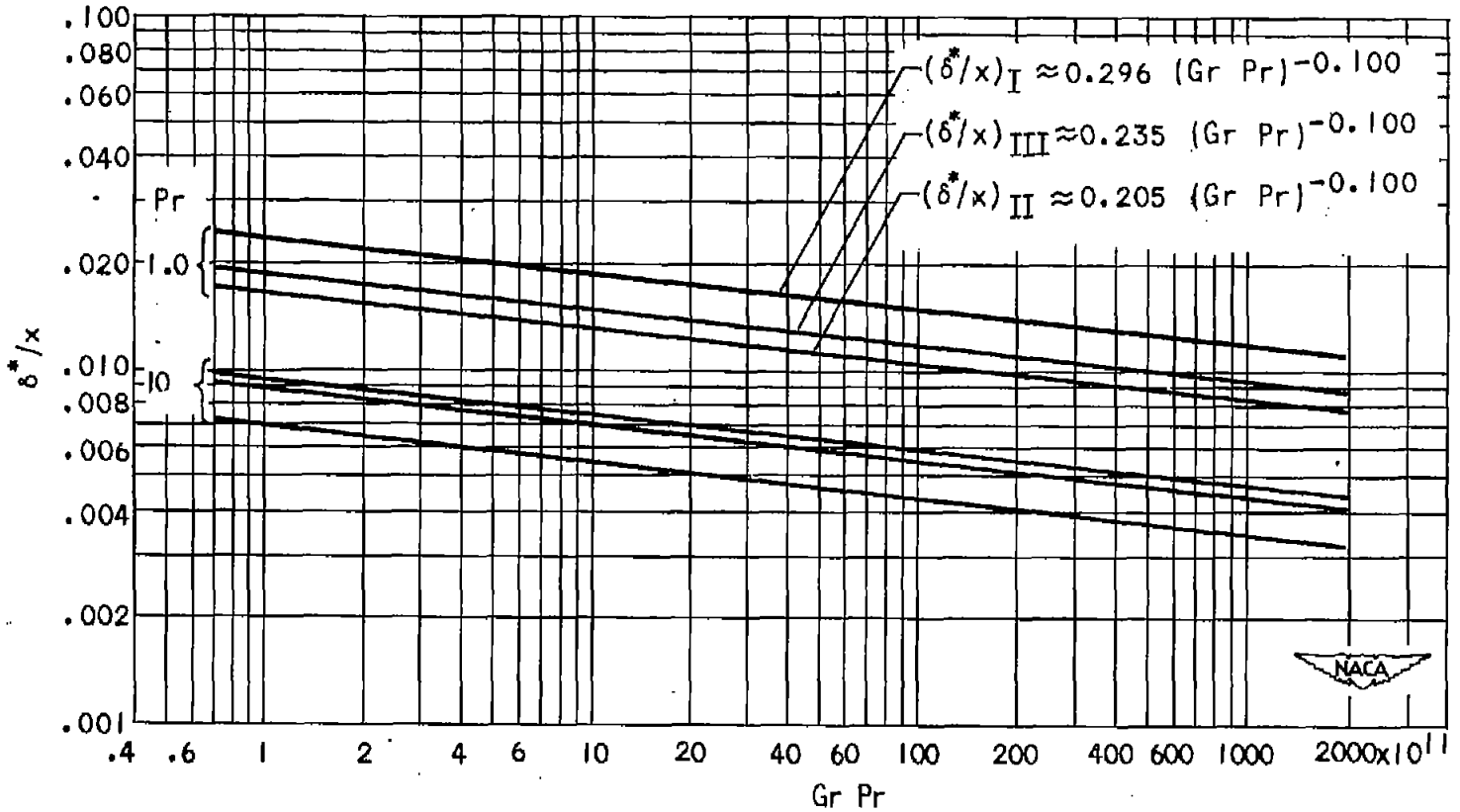

Figure 6. - Calculated displacement thickness δ^* of turbulent free-convection boundary layer plotted against product of Grashof number and Prandtl number.

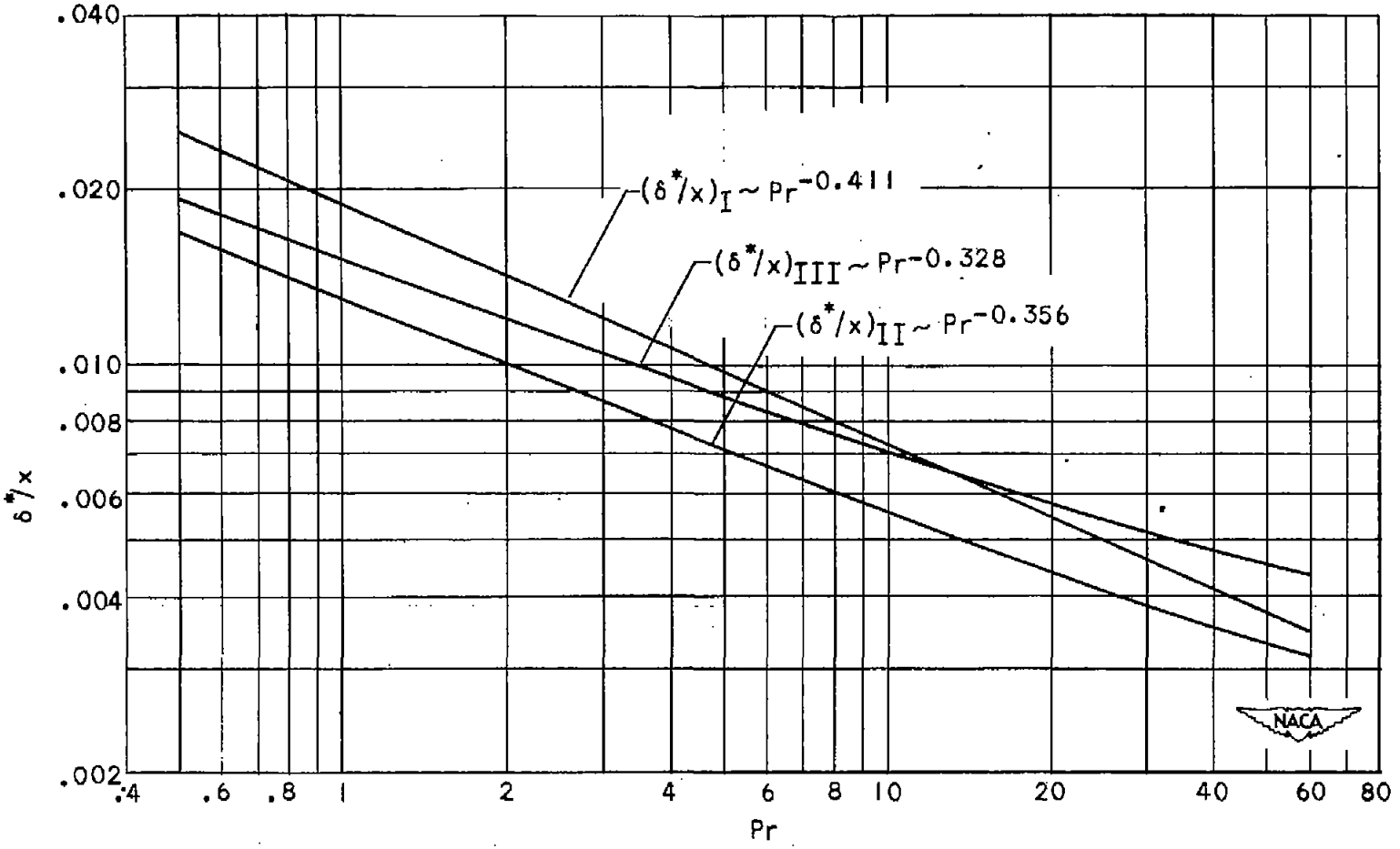

Figure 7. - Calculated displacement thickness δ^* of turbulent free-convection boundary layer plotted against Prandtl number. H proportional to $x^{1/5}$; (Gr Pr) = 10^{12}.

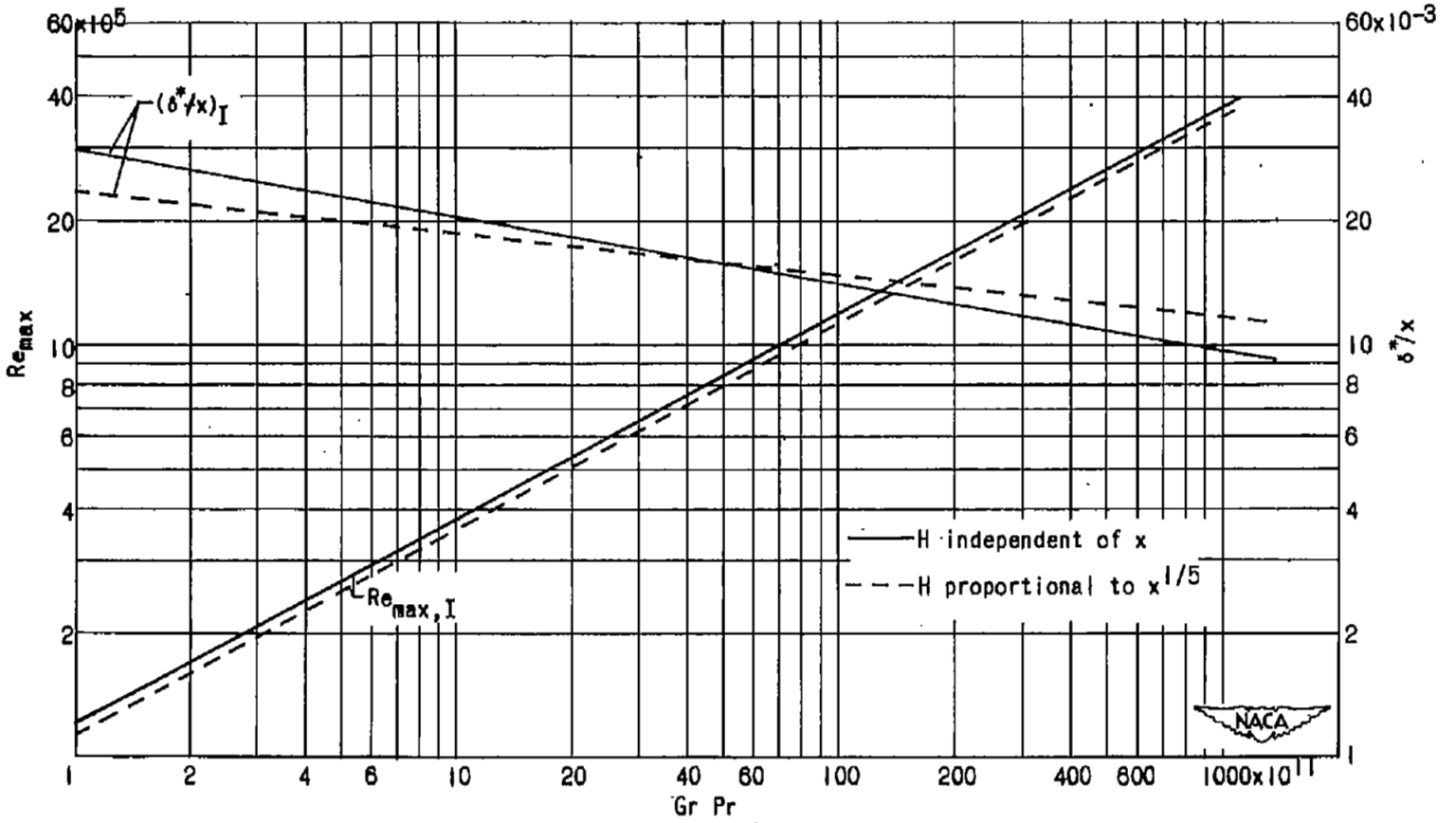

Figure 8. - Reynolds number Re_{max} characterizing maximum velocity in boundary layer and displacement thickness δ^* plotted against product of Grashof number and Prandtl number calculated with two assumptions for heat-transfer coefficient. Prandtl number = 1.0.

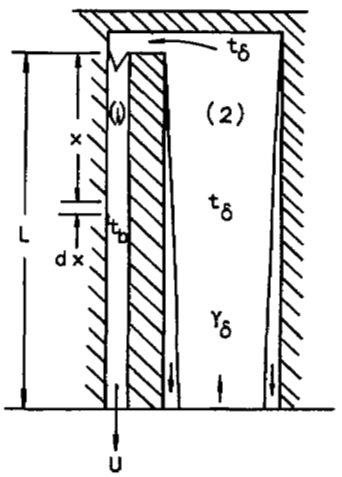

Figure 9. - Small-diameter hole (1) connected on top to large-diameter hole (2).

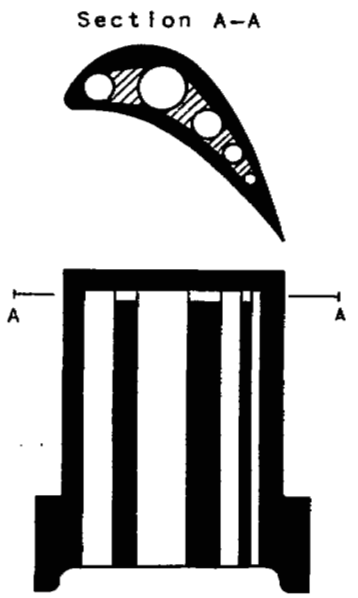

Figure 10. - Proposed arrangements of cooling passages in free-convection liquid-cooled turbine blades.

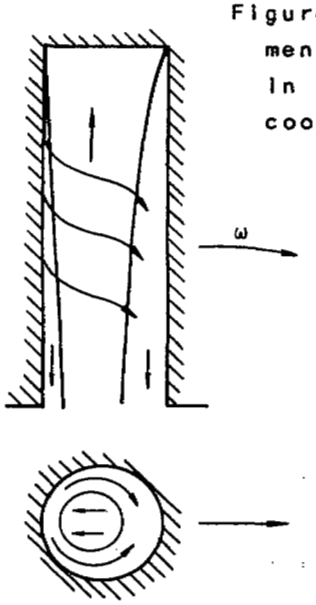

Figure 11. - Influence of Coriolis forces on free-convection flow in rotating hole with heated walls.

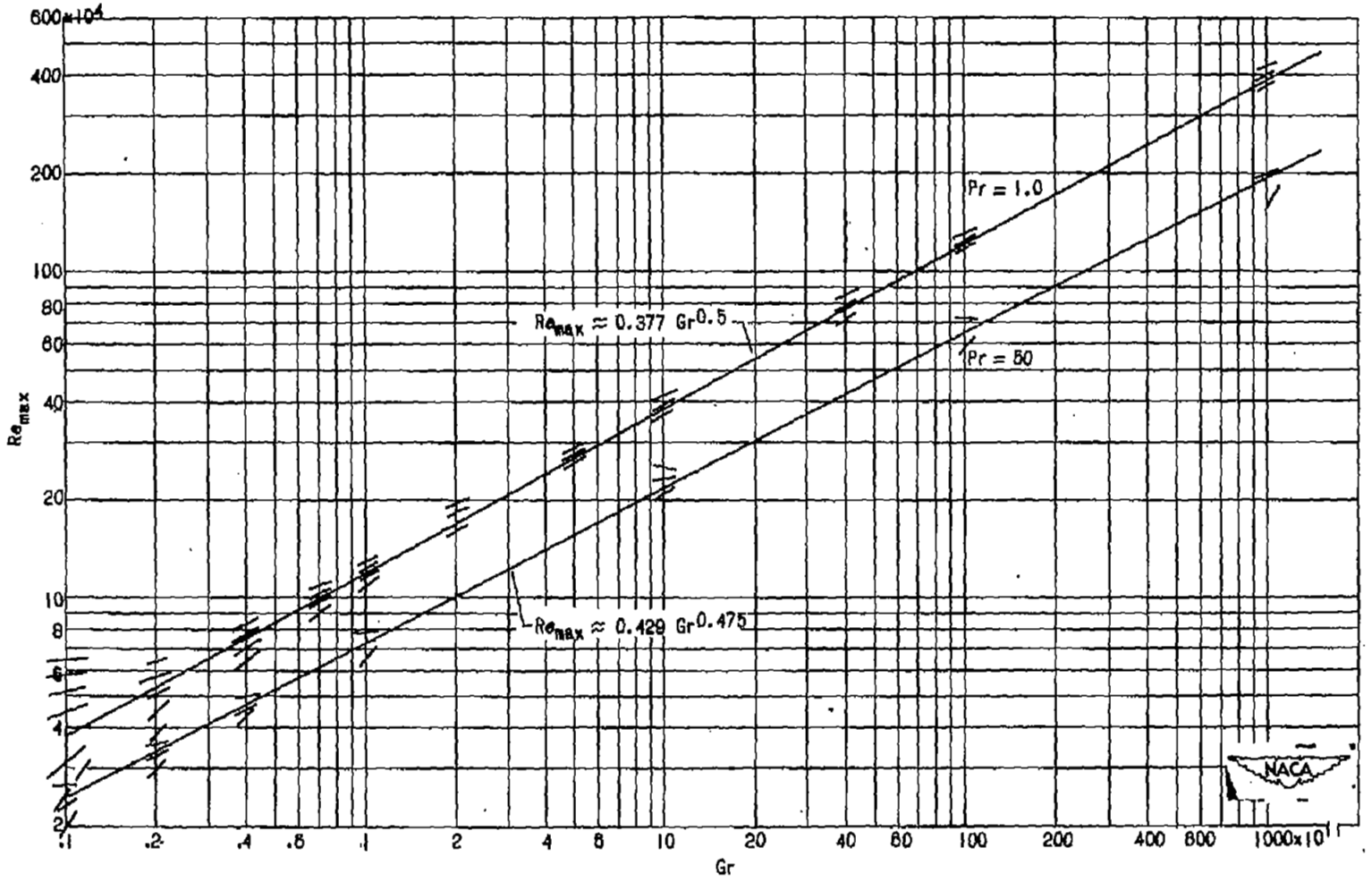

Figure 12. - Graphical solution of differential equation

$$\frac{d(Re_{max})}{d(Gr)} = \frac{0.0852}{Re_{max}} - \frac{0.0250\ Re_{max}^{2}\ Pr^{5/6}}{Gr^{17/12}}.$$